Article

Microscopic Description of the Polyamorphic Phases of Triphenyl Phosphite by Means of Multidimensional Solid-State NMR Spectroscopy

Jrgen Senker, Jan Sehnert, and Sascha Correll

J. Am. Chem. Soc., **2005**, 127 (1), 337-349• DOI: 10.1021/ja046602q • Publication Date (Web): 03 December 2004

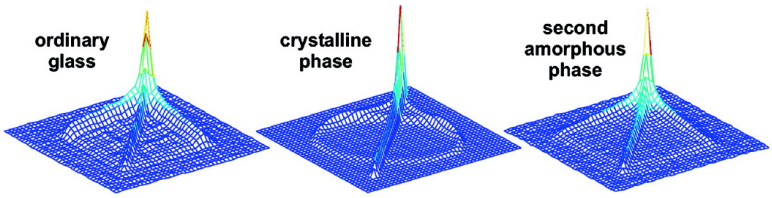

More About This Article

Additional resources and features associated with this article are available within the HTML version:

- Supporting Information
- Links to the 5 articles that cite this article, as of the time of this article download
- Access to high resolution figures
- Links to articles and content related to this article
- Copyright permission to reproduce figures and/or text from this article

View the Full Text HTML

J|A|C|S
ARTICLES
Published on Web 12/03/2004

Microscopic Description of the Polyamorphic Phases of Triphenyl Phosphite by Means of Multidimensional Solid-State NMR Spectroscopy

Jürgen Senker,* Jan Sehnert, and Sascha Correll

Contribution from the Department Chemie und Biochemie der Universität München, D-81377 München, Germany

Received June 9, 2004; E-mail: juergen.senker@cup.uni-muenchen.de

Abstract: The structural properties of a second, apparently amorphous phase (aII) of the molecular glass former triphenyl phosphite were studied by means of multidimensional solid-state NMR spectroscopy and X-ray diffraction. Phase aII was prepared by annealing the supercooled liquid in the temperature range 210 K $\leq T_a \leq$ 230 K. In addition to 1D ^{1}H and ^{31}P spectra and spin−lattice relaxation data, we used ^{31}P radio-frequency-driven spin-diffusion exchange spectroscopy to analyze the arrangement of neighboring TPP molecules on both a local and intermediate scale. For the first time, our results give a detailed microscopic description of phase aII. For $T_a >$ 223 K a nano- or microcrystalline material is formed, whereas for $T_a <$ 223 K phase aII is homogeneous and disordered. Our data strongly suggest that some of the TPP molecules in phase aII tend toward a parallel alignment. The regions, where the molecules preferentially align appear to be spatially separated and consist of only a few molecules. Whereas the mean cubic expansion of an individual region does not change within the experimental error, the percentage of correlated molecules increases with rising T_a. Based on our results, phase aII can consistently be described as a second liquid, where a part of the molecules exhibit structural correlations. The transformation of the supercooled liquid into phase aII is therefore considered as a liquid−liquid phase transition.

1. Introduction

Triphenyl phosphite (TPP), which forms a molecular glass, has recently attracted much attention because of its unusual phase behavior.[1−9] On cooling the ordinary fluid faster than 6 K/min, TPP first forms a supercooled liquid (phase aI) below the melting temperature $T_m \approx$ 290 K and then turns into a glass at $T_g =$ 205 K. If phase aI is annealed in the temperature range 210 K $\leq T_a \leq$ 230 K, a new phase (aII) develops, which appears to be amorphous based on X-ray powder diffraction studies.[10−12] Several groups have reported that the physical and rheological properties, such as density,[10−12] shear modulus,[1] sound velocity,[13] spin−lattice relaxation,[13,14] or heat capacity and enthalpy,[15−17] of phase aII differ significantly from both the supercooled liquid and the ordinary crystal. For these reasons, phase aII seems to be a second disordered state, which is stable compared to phase aI but metastable with respect to the crystal.

The existence of the phases aI and aII makes TPP a candidate for the phenomenon "polyamorphism".[2,3] Polyamorphism denotes the existence of at least two liquid or amorphous phases separated by first-order resembling phase transitions in an isotropic one-component system.[8,9] This idea is supported by theoretic models[18−20] and by MD simulations.[21−25] In both cases different condensed disordered phases are frequently found. The definition however excludes transitions

(1) Tanaka, H.; Kurita, R.; Mataki, H. *Phys. Rev. Lett.* **2004**, *92*, 025701/1−4.
(2) Tarjus, G.; Alba-Simionesco, C.; Grousson, M.; Viot, P.; Kivelson, D. *J. Phys: Condens. Matter* **2003**, *15*, S1077−S1084.
(3) Kivelson, D.; Tarjus, G. *J. Non-Cryst. Solids* **2002**, *307−310*, 630−636.
(4) Hédoux, A.; Guinet, Y.; Descamps, M.; Lefèbvre, J. *Phase Transitions* **2003**, *76*, 831−836.
(5) Guinet, Y.; Denicourt, T.; Hédoux, A.; Descamps, M. *J. Mol. Struct.* **2003**, *651−653*, 507−517.
(6) Hédoux, A.; Dore, J.; Guinet, Y.; Bellissent-Funel, M. C.; Prevost, D.; Descamps, M.; Grandjean, D. *Phys. Chem. Chem. Phys.* **2002**, *4*, 5644−5648.
(7) Hédoux, A.; Guinet, Y.; Foulon, M.; Descamps, M. *J. Chem. Phys.* **2002**, *116*, 9374−9382.
(8) Senker, J.; Rössler, E. *J. Phys. Chem. B* **2002**, *106*, 7592−7595.
(9) Senker, J.; Rössler, E. *Chem. Geol.* **2001**, *174*, 143−156.
(10) Demirjian, B. G.; Dosseh, G.; Chauty, A.; Ferrer, M.-L.; Morineau, D.; Lawrence, C.; Takeda, K.; Kivelson, D.; Brown, S. *J. Phys. Chem. B* **2001**, *105*, 2107−2116.
(11) Hédoux, A.; Hernandez, O.; Lefèbvre, J.; Guinet, Y.; Descamps, M. *Phys. Rev. B* **1999**, *60*, 9390−9395.
(12) Cohen, I.; Ha, A.; Zhao, X.; Lee, M.; Fischer, T.; Strouse, M. J.; Kivelson, D. *J. Phys. Chem.* **1996**, *100*, 8518−8526.
(13) Wiedersich, J.; Kudlik, A.; Gottwald, J.; Benini, G.; Roggatz, I.; Rössler, E. *J. Phys. Chem. B* **1997**, *101*, 5800−5803.
(14) Dvinskikh, S.; Benini, G.; Senker, J.; Vogel, M.; Wiedersich, J.; Kudlik, A.; Rössler, E. *J. Phys. Chem. B* **1999**, *103*, 1727−1737.
(15) Johari, G. P.; Ferrari, C. *J. Phys. Chem. B* **1997**, *101*, 10191−10197.
(16) Mizukami, M.; Kobashi, K.; Hanaya, M.; Oguni, M. *J. Phys. Chem. B* **1999**, *103*, 4078−4088.
(17) van Miltenburg, K.; Blok, K. *J. Phys. Chem.* **1996**, *100*, 16457−16459.
(18) Sperl, M. Asymptotic laws near higher-order glass-transition singularities. PhD Thesis, TU München, 2003.
(19) Tanaka, H. *J. Phys.: Condens. Matter* **1999**, *11*, L159−L168.
(20) Tejero, C. F.; Baus, M. *Phys. Rev. E* **1998**, *57*, 4821−4823.
(21) Senda, Y.; Shimojo, F.; Hoshino, K. *J. Non-Cryst. Solids* **2002**, *312−314*, 80−84.
(22) Morishita, T. *Phys. Rev. B* **2002**, *66*, 054204/1−7.
(23) Saika-Voivod, I.; Poole, P. H.; Sciortino, F. *Nature* **2001**, *412*, 514−517.
(24) Wu, C. J.; Glosli, J. N.; Galli, G.; Ree, F. H. *Phys. Rev. Lett.* **2002**, *89*, 135701/1−4.
(25) Poole, P. H.; Grande, T.; Angell, C. A.; McMillan, P. F. *Science* **1997**, *275*, 322−323.

which are accompanied by a change of symmetry, such as transformations between crystalline polymorphs or liquids and liquid crystals. Polyamorphic phase behavior is rarely observed experimentally for two main reasons. First, a large pressure and temperature range has to be covered, which still requires challenging experiments. Second, since such transitions are expected to occur in a pT-region where most liquids are metastable, polyamorphism may often be masked by crystallization. Up to now only a few examples have been reported, including compounds which form three-dimensional networks such as H_2O,[26−29] SiO_2,[23,30,31] GeO_2,[32] silicon,[33] and carbon,[24] as well as compounds which have the tendency to exist in different polymeric structures, such as phosphorus[34−36] or sulfur.[37] However, TPP is unique, since the strongest packing forces are van der Waals interactions.[38]

For most of these examples the nature of the polyamorphic phases is unclear. This is probably generally due to the problem of structure determination in disordered materials. In contrast to crystalline systems, where even large and complicated structures can be solved in routine treatments by single-crystal diffraction, ab initio structure determination in amorphous materials is much more complex due to the lack of periodicity in such phases.[39] Although a large variety of spectroscopic techniques such as IR/Ra,[4] XANES,[40] or NMR,[41] as well as wide and small angle scattering experiments with X-ray,[4,28] neutron,[28] or synchrotron[34] radiation, may be used to obtain structural details in amorphous materials, the information obtained either is limited to a local scale (<∼10 Å) or gives insight into order phenomena on a mesoscopic scale (>∼100 Å).[9] In contrast, only very few techniques can investigate the intermediate range. Obtaining insight into this range is often crucial for the characterization of specific building blocks, as well as for the analysis of simultaneous and cooperative ordering phenomena like phase transitions, self-organization, or nucleation.[3,29,42,43] Therefore it is often not possible to form a unique picture of structural properties in disordered phases, which results in a variety of structure models explaining the experimental data. The different phases of TPP have been actively investigated by several groups which has resulted in a large variety of different structure models being proposed. These are summarized in the following discussion. It is interesting to note that until now this matter has been the cause of a lively debate where no consensus has been reached so far. Furthermore, it should be stressed that it is not only the structural arrangement of the TPP molecules in phase aII that is a controversial topic but also its homogeneity.

On the basis of X-ray,[4,11] synchrotron,[11] neutron,[6,44] and Raman[4,5,45−47] scattering experiments, Decamps, Hédoux, and co-workers proposed that phase aII is a mixture of the supercooled liquid and nanocrystals with the structural properties of the ordinary crystal.[38,48] The fraction of nontransformed liquid strongly depends on the aging temperature T_a. Below 224 K, where nucleation is much faster than crystal growth, the crystallization process stops when the liquid is saturated with seed crystals.[7] Phase aII appears as a stable phase at constant temperature, although it would consist of small nanocrystals and nontransformed phase aI. Above 224 K, the rates of nucleation and crystal growth are of the same order and the transformation process can proceed to completion resulting in a homogeneous phase consisting of nano- and microcrystals, respectively.

The results of Oguni et al.[16] and Tanka et al.[1] as well as Rössler, Senker, and co-workers[8,9,14] favor the picture of phase aII as a homogeneous liquid. The TPP molecules in phase aII exhibit pronounced reorientation dynamics at elevated temperatures, as was shown using dielectric spectroscopy[14,16] and ^{31}P stimulated echo experiments.[14] Although the loss of correlation in phase aII takes place on a longer time scale compared with the one in the supercooled liquid,[14,16] the molecular reorientation processes are comparable. Measurements of the density fluctuations during transformation of phase aI into phase aII with optical microscopy[1] revealed a time dependent behavior characteristic for a spinodal decomposition above $T_{SD} \approx 216$ K as it is typical for an underlying liquid−liquid transition.[1] After long annealing times the density fluctuations vanish and no phase boundaries can be observed. This indicates that phase aII is homogeneous, which is in contrast to the findings of Decamps and Hédoux.

Finally, Johari and Ferrari suggested that phase aII might be a liquid or plastic crystalline state.[15] The possibility of a plastic crystal was also proposed by Kivelson et al.,[10] who interpreted both the occurrence of a fluidlike resonance in the ^1H solid-state NMR spectra and the increase of the specific heat[17] during the heating of phase aII to a temperature between 228 and 231 K as the premelting of phase aII. Since only ordered systems such as crystals or plastic crystals melt, phase aII should therefore exhibit some crystal-like order. Considering the molecular dynamics of the TPP molecules,[14] Kivelson et al. assumed that phase aII might be a plastic crystal.[10] However, to explain the absence of Bragg scattering the crystallite size has to be smaller than ∼10 nm. Tarjus, Alba-Simionesco, and Kivelson[2,3] follow a similar approach, whereby they describe phase aII as being a highly defect-ordered crystal as would be

(26) Finney, J. L.; Bowron, D. T.; Soper, A. K.; Loerting, T.; Mayer, E.; Hallbruker, A. *Phys. Rev. Lett.* **2002**, *89*, 205503/1−4.
(27) Finney, J. L.; Hallbruker, A.; Kohl, I.; Soper, A. K.; Bowron, D. T. *Phys. Rev. Lett.* **2002**, *88*, 225503/1−4.
(28) Tulk, C. A.; Benmore, C. J.; Urquidi, J.; Klug, D. D.; Neuefeind, J.; Tomberli, B.; Egelstaff, P. A. *Science* **2002**, *297*, 1320−1323.
(29) Mishima, O.; Stanley, H. *Nature* **1998**, *396*, 329−335.
(30) Mukherjee, G. D.; Vaidya, S. N.; Sugandhi, V. *Phys. Rev. Lett.* **2001**, *87*, 195501/1−4.
(31) Lacks, D. *J. Phys. Rev. Lett.* **2000**, *84*, 4629−4632.
(32) Smith, K. H.; Shero, E.; Chizmeshya, A.; Wolf, G. H. *J. Chem. Phys.* **1995**, *102*, 6851−6857.
(33) Deb, S. K.; Wilding, M.; Somayazulu, M.; McMillan, P. F. *Nature* **2001**, *414*, 528−530.
(34) Monaco, G.; Falconi, S.; Crichton, W. A.; Mezouar, M. *Phys. Rev. Lett.* **2003**, *90*, 255701/1−4.
(35) Katayama, Y. *J. Non-Cryst. Solids* **2002**, *312−314*, 8−14.
(36) Katayama, Y.; Mizutani, T.; Utsumi, W.; Shimomura, O.; Yamakata, M.; Funakoshi, K. *Nature* **2000**, *403*, 170−173.
(37) Brazhkin, V. V.; Popova, S. V.; Voloshin, R. N. *Physica B* **1999**, *265*, 64−71.
(38) Senker, J.; Lüdecke, J. *Z. Naturforsch.* **2001**, *56b*, 1089−1099.
(39) Senker, J.; Seyfarth, L.; Voll, J. *Solid State Sci.* **2004**, 1039−1052.
(40) Hagenmayer, R. M.; Müller, U.; Benmore, C. J.; Neuefeind, J.; Jansen, M. *J. Mater. Chem.* **1999**, *9*, 2865−2869.
(41) van Wüllen, L.; Müller, U.; Jansen, M. *Chem. Mater.* **2000**, *12*, 2347−2352.
(42) Jansen, M.; Jäschke, B.; Jäschke, T. *Struct. Bonding* **2002**, *101*, 137−191.
(43) Richet, P.; Gillet, P. *Eur. J. Mineral.* **1997**, *9*, 907−933.
(44) Hédoux, A.; Derollez, P.; Guinet, Y.; Dianoux, A. J.; Descamps, M. *Phys. Rev. B* **2001**, *63*, 144202/1−8.
(45) Hédoux, A.; Denicourt, T.; Guinet, Y.; Carpentier, L.; Descamps, M. *Solid State Commun.* **2002**, *122*, 373−378.
(46) Hédoux, A.; Guinet, Y.; Descamps, M. *J. Raman Spectrosc.* **2001**, *32*, 677−688.
(47) Hédoux, A.; Guinet, Y.; Descamps, M.; Bénabou, A. *J. Phys. Chem. B* **2000**, *104*, 11774−11780.
(48) Hernandez, O.; Hédoux, A.; Lefèbvre, J.; Guinet, Y.; Descamps, M.; Papoular, R.; Masson, O. *J. Appl. Crystallogr.* **2002**, *35*, 212−219.

expected from their theory of frustration limited domains.[10] According to their analysis of the low-Q region of the powder neutron diffraction data,[49] the lattice parameters of this defect-ordered state are roughly 80 Å, and the crystallite size was estimated to be 150−200 Å. Since the lattice parameters of the ordinary crystal[38] ($a = b = 37.887(1)$ Å and $c = 5.7567(2)$ Å) differ significantly from the above-mentioned value, the structural arrangement of the defect-ordered crystal should differ from that of the normal crystal.

The aim of the work presented here is to gain a deeper insight into structural properties of phase aII, since, as being discussed above, even the combined use of several different techniques could so far not provide a consistent picture. Taking a closer look at the models discussed above, this is probably caused by a lack of reliable information regarding ordering phenomena in an intermediate region. Recent developments in the field of structure determination using solid-state NMR[39,41,50−52] demonstrate that modern sequences allow access to structural details on this crucial scale. We therefore chose radio-frequency-driven (rf-driven) spin-diffusion exchange spectroscopy to investigate both of the amorphous phases of TPP more closely. Rf-driven exchange spectra give information about both the orientation and distance correlations of neighboring molecules or building blocks independent of the degree of order of the sample.[39,52,53]

By applying this technique to the crystalline phase of TPP[39] we were recently able to obtain the $\bar{3}$-fold symmetry of the molecular arrangement in the crystal and to determine the distance between neighboring molecules as 8.1 Å. This is very close to the 8.09 Å found by single-crystal X-ray diffraction.[38] By applying this technique to both amorphous phases of TPP, we were able to obtain information which was not available using any other analytical method. It is worth noting that the NMR experiments used in the work presented here can easily be used to unravel microscopic properties in other systems as well. For example, it would also be interesting to investigate lipid bilayers containing peptides, where aligned and unaligned components were observed in neighboring domains.[54−56]

2. Experimental Methods

Triphenyl phosphite (TPP) was purchased from Merck (Germany) with a purity greater than 98%. The samples for NMR experiments were prepared by filling each standard NMR glass tube (Ø = 5 mm) with roughly 250 mm^3 of liquid TPP. After degassing with a standard freeze and pump technique to prevent nucleation due to gas evolution, the tubes were sealed off under vacuum. Afterward the samples were characterized using ^{1}H, ^{13}C, and ^{31}P liquid NMR spectroscopy to reveal that the main impurity is triphenyl phosphate (∼2 atom %).

Recently TPP has been doped with different impurities such as phosphoric acid, benzene, hexamethyl benzene, or phenol, and it could be shown that an impurity level up to ∼10 atom % does not influence the characteristics of the transition of the supercooled liquid into phase aII.[8,10,14] Therefore, purification of our samples was not necessary. The samples were mounted in a commercial CP double resonance probe (Bruker) equipped with a 5 mm solenoid coil. The probe allows the sample temperatures to be adjusted between 170 and 470 K using a constant flow of cold, dry nitrogen. Heater power and sample temperature were controlled via a BVT 3000 unit (Bruker). The absolute temperature was calibrated using the chemical shift thermometer $Pb(NO_3)_2$[57] and is believed accurate within ±2 K. The temperature stability is better than ±0.2 K.

^{1}H and ^{31}P wide-line NMR experiments were carried out with a conventional DSX Avance impulse spectrometer (Bruker, Germany) operating with resonance frequencies of 500 and 202.5 MHz, respectively. For all 1D and 2D ^{31}P NMR experiments, broadband proton decoupling was applied using a TPPM sequence during the evolution and acquisition periods.[58] The rf-field strength of the ^{1}H channel was adjusted to 80 kHz, and every 5.8 μs the pulse phase was switched about ±7.5°. Using continuous wave decoupling a similar decoupling efficiency could be reached.

We recorded 1D spectra for both nuclei, using a solid-echo for ^{1}H and a Hahn-echo pulse sequence for ^{31}P. In both cases the 90° pulse length was adjusted to values between 2.5 and 3.0 μs. The interpulse delay was set to 10 μs for the solid-echo spectra and to 30 μs in the case of the Hahn-echo measurements. Spin−lattice relaxation time constants T_1 were measured by applying a saturation block consisting of ten 90° pulses separated by 2−5 ms ahead of the echo sequences. To prevent spectral distortions, we estimated the shortest recovery delay possible based on the magnitude of T_1. Furthermore, the magnitude of the ^{31}P spin−lattice relaxation constant allowed us to distinguish between both amorphous phases and the crystalline modification of TPP, as has been demonstrated in refs 9 and 14.

To investigate the local arrangement of the TPP molecules in both amorphous phases we used radio-frequency-driven spin-diffusion[53] exchange spectroscopy.[39] The 2D ^{31}P exchange spectra were recorded with recently developed pulse sequences.[39] After preparation of transversal ^{31}P magnetization with ^{1}H−^{31}P cross polarization[59,60] (contact time 3 ms), the phosphorus nuclei were allowed to exchange polarization by applying a composite spin-lock with a WALTZ17 sequence.[53] The rf-field strength was adjusted to 125 kHz, and the last spin-locking pulse α[39] was fixed to a $\pi/4$ pulse. Since the composite spin-lock already removes heteronuclear dipole interactions, no additional proton decoupling was applied during the mixing time. For further information concerning pulse phases, phase cycles, pulse lengths, or other details during the spin-lock, the reader is referred to ref 39. Depending on the mixing time t_m the 2D spectra were obtained with 128−256 increments of the first evolution period in steps of 4 μs and either 16 or 32 repetitions for each increment. To obtain pure absorption spectra we used time-proportional phase incrementation in the t_1 domain and transformed the collected data matrix $s(t_1,t_2)$ with a complex Fourier transformation in the t_2 domain and a cosine Fourier transformation in the t_1 domain.

As demonstrated in ref 39 the distances between neighboring molecules can be estimated from the evolution of the ratio I_D/I_C for a series of 2D spectra as a function of t_m. I_D and I_C denote the diagonal and the cross intensity of a 2D spectrum, respectively. For this purpose, the normalized zero-quantum line shape at $\omega = 0$ under spin-locking conditions $F_{rf}(0)$ has to be determined separately. Since $F_{rf}(\omega)$ cannot be measured directly, it has to be either calculated or estimated experimentally.[52] For the work presented here we derived $F_{rf}(0)$ from $F(\omega)$, which is the normalized zero-quantum line shape in the laboratory coordinate system.[61] If the single-quantum line shape $f^{\omega_{CS}}(\omega)$ is homogeneous and dominated by the homonuclear ^{31}P dipole interaction,

(49) Alba-Simionesco, C.; Tarjus, G. *Europhys. Let.* **2001**, *52*, 297−303.
(50) Ratai, E.-M.; Janssen, M.; Epping, J. D.; Chan, J. C. C.; Eckert, H. *Phys. Chem. Glasses* **2003**, *44*, 45−53.
(51) Jäger, C.; Hartmann, P.; Witter, R.; Braun, M. *J. Non-Cryst. Solids* **2000**, *263−264*, 61−72.
(52) Robyr, P.; Tomaselli, M.; Straka, J.; Grob-Pisano, C.; Suter, U. W.; Meier, B. H.; Ernst, R. R. *Mol. Phys.* **1995**, *84*, 995−1020.
(53) Meier, B. H. In Advances in Magnetic and Optical Resonance; Academic Press: 1994; Vol. 18, pp 1−116.
(54) Hallock, K. J.; Lee, D.-K.; Omnaas, J.; Mosberg, H. I.; Ramamoorthy, A. *Biophys. J.* **2002**, *83*, 1004−1013.
(55) Henzler Wildman, K. A.; Lee, D.-K.; Ramamoorthy, A. *Biochemistry* **2003**, *42*, 6545−6558.
(56) Hallock, K. J.; Lee, D.-K.; Ramamoorthy, A. *Biophys. J.* **2003**, *84*, 3052−3060.
(57) Bielecki, A.; Burum, D. *J. Magn. Reson. A* **1995**, *116*, 215−220.
(58) Bennett, A. E.; Rienstra, C. M.; Auger, M.; Lakshmi, K. V.; Griffin, R. G. *J. Chem. Phys.* **1995**, *103*, 6951−6958.
(59) Shekar, S. C.; Ramamoorthy, A. *Chem. Phys. Lett.* **2001**, *342*, 127−134.
(60) Shekar, S. C.; Lee, D.-K.; Ramamoorthy, A. *J. Magn. Reson.* **2002**, *157*, 223−234.

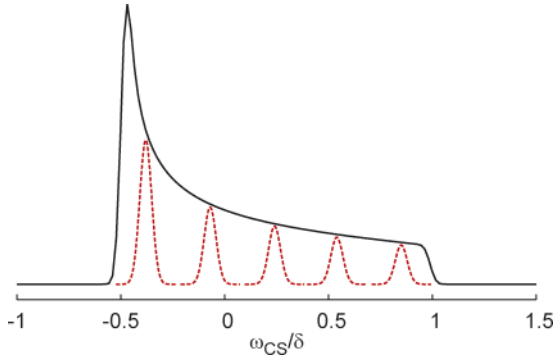

Figure 1. Scheme of a 1D solid-state NMR spectrum for a powder sample dominated by the anisotropic chemical shift interaction with the anisotropy parameter δ. The spectrum consists of a superposition of single-quantum line shapes $f^{\omega_{CS}}(\omega)$ (dashed lines). Each single-quantum spectrum represents a specific orientation of a TPP molecule toward B_0.

$F(\omega)$ may be estimated by convoluting $f^{\omega_{CS}}(\omega)$ for all possible combinations of ω_{CS}. ω_{CS} represents the position of $f(\omega)$ in the 1D solid-state spectrum, which is dominated by the chemical shift interaction (see Figure 1).

Since our experiments were carried out using broadband proton decoupling, $f^{\omega_{CS}}(\omega)$ is exclusively influenced by $^{31}P-^{31}P$ dipolar couplings. Although the structural arrangement of the TPP molecules varies from phase to phase, all three modifications of TPP have in common that the phosphorus nuclei are uniformly distributed. Thus a spin i is surrounded by many other spins with equally distributed distances and no preferred orientation. $f^{\omega_{CS}}(\omega)$ for the spin i is, therefore, caused by a considerable number of extraneous ^{31}P nuclei. Due to the steric hindrance of the phenyl groups, the shortest PP distances are limited to roughly 6 Å and the coupling between all spins is moderate. If it is further considered that each phosphorus atom of one phase has a similar surrounding, the expectation that $f^{\omega_{CS}}(\omega)$ is homogeneous and exhibits no large variations neither for different isochromates nor for spin pairs belonging to one isochromate is supported. We, therefore, assume that $F(0)$ and $F_{rf}(0)$ are similar for all spin pairs ij and do not vary as a function of the PP distances of a specific spin pair. For the crystalline phase of TPP an analysis of separated local field spectra proved that the width of $f^{\omega_{CS}}(\omega)$ does not vary by more than ~10% for different isochromates.[39]

Thus it is sufficient to use the mean single-quantum spectrum $\langle f(\omega)\rangle$ for the calculation of the zero-quantum line shape. $F(\omega)$ then results as the convolution of $\langle f(\omega)\rangle$ with itself. $\langle f(\omega)\rangle$ can be extracted as the Fourier transform of the decay of the echo top $M(\tau)$ of a Hahn-echo experiment as a function of the interpulse delay $\tau/2$. As a result of broadband proton decoupling during the acquisition, the intensity of $M(\tau)$ is damped only due to spin−spin relaxation caused by the homonuclear dipolar coupling between the phosphorus nuclei. $F(\omega)$ can then be calculated by the following:

$$F(\omega) = \frac{FT(M^2(\tau))}{\int FT(M^2(\tau))\, d\omega} \quad (1)$$

Taking into account that the width of a homogeneous line is proportional to the square root of the second, $F_{rf}(0)$ results in

$$F_{rf}(0) = s^{-1} \cdot F(0) \quad (2)$$

with s being the scaling factor of the dipolar coupling under spin-locking conditions.

X-ray powder diffraction patterns were collected with a Stadi P diffractometer (Stoe, Germany) working in Debye−Scherrer geometry using Cu Kα1 radiation ($\lambda = 1.5406$ Å). The diffractometer is equipped with a 600 Series Cryostream Cooler (Oxford Cryosystems, United Kingdom). After temperature calibration with standard samples[62] an absolute temperature accuracy of ±2 K was reached. The liquid was sealed in glass capillaries (Ø = 0.5 mm) at room temperature.

For both the solid-state NMR and X-ray diffraction experiments the samples were first cooled with a rate of 6 K/min to 190 K, which is well below the glass transition temperature $T_g = 204$ K of TPP. To equilibrate the samples they were maintained at this temperature for 2 h before performing any other action. For the annealing experiments, the samples were heated from 190 K with 20 K/min to a specific annealing temperature T_a in the range of 212 K ≤ T_a ≤ 231 K. At T_a the samples were tempered for up to 2 d depending on the magnitude of T_a. In addition, we measured 1D ^1H and ^{31}P NMR spectra while heating the sample continuously with a small but constant rate of 0.3 K/min. For such experiments the recovery delay was fixed at 20 s and the phase cycling was reduced to four steps for both the solid- and Hahn-echo sequences.

3. Results

The homogeneity of phase aII is a controversial topic in the literature[1,4,5,9,13,14,45,46] (section 1). To gain further insight we at first studied the transformation of the supercooled liquid into phase aII by means of ^{31}P spin−lattice relaxation. In the past this technique has been proven to be a sensitive probe for investigating the dynamic properties of materials on a local scale (r_p < 10 Å).[9,13,14] The probe volume is confined to a small area because of the usually large chemical shift anisotropy of the phosphorus nuclei, which efficiently quenches spin diffusion in the laboratory coordinate system. This situation is not to be confused with the rf-driven spin-diffusion exchange experiments we will present below, where the spin-diffusion rates are enhanced by locking the magnetization in the rotating coordinate system.

We followed the transformation at different annealing temperatures T_a by continuously sampling the recovery of magnetization after a saturation sequence. For homogeneous materials the relaxation function Φ can be described by a stretched exponential as given in eq 3.

$$\Phi(t) = \frac{M_0 - M(t)}{M_0} = e^{(-t/T_1)^b} \quad (3)$$

T_1 denotes the characteristic time constant of the relaxation, and b is the stretching factor. In an ordered molecular material, b usually is close to 1, demonstrating that all molecules relax with an equal rate. For example, in the crystalline phase of TPP, the ^{31}P resonance relaxes with $T_1 = 276(2)$ s and $b = 0.970(8)$ at 200 K. For a disordered material the vicinity of a molecule varies slightly and the relaxation time constant has to be described by a distribution. This leads to a stretching factor b of values smaller than 1, the magnitude of b depending on the structural disorder. In the case of ^{31}P spin−lattice relaxation in molecular glasses, the nonexponentiality is not pronounced and b is usually found within 0.8 ≤ b ≤ 1.[14] The structural glass of TPP for example exhibits a relaxation constant $T_1 = 33.6(3)$ s and a stretching factor $b = 0.910(7)$ at 200 K and thus relaxes roughly 1 order of magnitude faster compared to the crystal at the same temperature. A mixture of the supercooled liquid and a crystalline material, even if nanocrystalline, will give rise to a biexponential Φ characterized by two time constants and

(61) Kubo, A.; McDowell, C. *J. Chem. Phys.* **1988**, *89*, 63−70.
(62) Tomaszewski, P. E. *Phase Transitions* **1992**, *38*, 127−220.

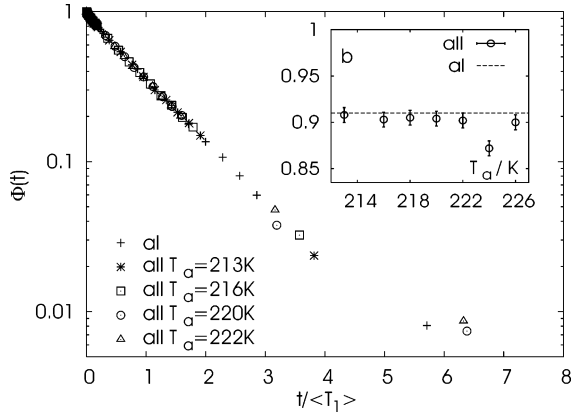

Figure 2. Relaxation function Φ for phases aI and aII measured at 200 K. Phase aII was prepared at different T_a as described in the text and cooled to 200 K before data collection. For a better comparison, the data are normalized to unit relaxation strength by dividing t by $\langle T_1 \rangle$. The inset depicts the stretching factor b for the same experiments.

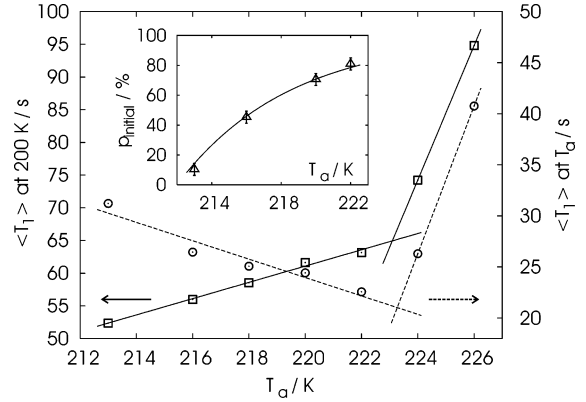

Figure 3. Mean relaxation times $\langle T_1 \rangle$ for phase aII prepared at different T_a. The open circles (right y-axis) represent measurements carried out directly after completed transformation at T_a. The open squares (left y-axis) are $\langle T_1 \rangle$ values for the same samples after cooling to 200 K. The inset shows the part of TPP molecules relaxing with a T_1 of several hundred seconds 10 min after heating the structural glass to T_a.

stretching factors. In contrast to that, for a homogeneous scenario one set of parameters will be sufficient.

Our findings during the transformation process support recently published results[9,13,14] and can be summarized as follows: At the beginning of the transformation a biexponential relaxation was observed as depicted in Figure 4 of ref 13. The smaller T_1 is characteristic for the supercooled liquid (3 s $\leq T_1 \leq$ 10 s), whereas with a magnitude of several hundred seconds the larger T_1 represents immobilized TPP molecules. During the aging of the sample, the slow relaxation process becomes faster and the fast process slows down until, after a characteristic time which strongly depends on T_a, both relaxation processes merge into one, slowly approaching a limit for T_1.

Figure 2 depicts the relaxation function of phase aII after complete transformation at different T_a. For comparison, a data set for the structural glass (aI) was added. All measurements were carried out at 200 K. The data were refined using eq 3, and the stretching factor b is given in the inset of Figure 2. The similar nature of the normalized Φ, which is also shown in the nearly identical stretching factors b for all T_a, clearly demonstrates that, with annealing times chosen appropriately long, all TPP molecules of phase aII exhibit a similar relaxation strength. This result is in complete agreement with considering phase aII as homogeneous but in disagreement with the proposition of describing phase aII as a mixture of the supercooled liquid and nanocrystals.

The mean relaxation constants $\langle T_1 \rangle$ calculated according to[14]

$$\langle T_1 \rangle = \frac{T_1 \cdot \Gamma(1/b)}{b} \tag{4}$$

are depicted in Figure 3 for two scenarios. The first data set was recorded directly after a completed transformation at T_a (open circles and right y-axis of Figure 3), whereas the second series was determined after cooling the transformed sample to 200 K (open squares and left y-axis of Figure 3).

For both series, a discontinuity around 223 K was observed as well as a strong increase of $\langle T_1 \rangle$ for $T_a >$ 223 K. At these temperatures the TPP molecules become increasingly immobile due to the formation of nano- and microcrystalline materials. In this context the considerably smaller stretching factor b for T_a = 224 K (inset of Figure 2) should be mentioned, which suggests that for this annealing temperature a mixture of phase aII and a nanocrystalline material is formed. However, for T_a = 226 K the sample already appears to be homogeneous again.

For $T_a <$ 223 K, $\langle T_1 \rangle$ decreases with increasing T_a if measured directly at the transition temperature. This indicates that the tumbling of the TPP molecules about large angles becomes faster when a larger T_a is chosen. This behavior was also observed by Rössler et al.[9,14] by means of dielectric spectroscopy and stimulated echo experiments. On the other hand, the increase of $\langle T_1 \rangle$ as a function of T_a for data sets collected at 200 K demonstrates that the residual mobility of the TPP molecules (at 200 K large angle reorientations of the TPP molecules are quenched) decreases with increasing T_a. This observation agrees with the results of Oguni and co-workers,[16] who propose that phase aII develops a structural correlation as a function of T_a. Apparently, the higher mobility of the TPP molecules of phase aII for larger T_a enables the molecules to relax more freely and settle in a state of higher structural order.

In this context, the biexponential relaxation at the beginning of the transformation should also be discussed. In accordance with Tanaka[1] and Kivelson,[12,63] this behavior can be understood only by assuming an inhomogeneous phase with domains where the molecules are packed more closely than in other parts of the sample. Due to their denser packing, the molecules in these domains lose their ability to tumble and therefore relax with a time constant of several hundred seconds. The inset of Figure 3 shows the percentage of such immobilized TPP molecules ($p_{initial}$) at different T_a. At an annealing temperature of 213 K only 10% of the TPP molecules are part of these domains, whereas at T_a = 222 K the denser parts take 80%. The expansion of these domains must be at least in the order of several nanometers, and only a few are formed at low temperatures. It is very likely that phase aII starts to grow from such regions of density fluctuations in the sample. If the length of these fluctuations is comparable for all transition temperatures, the increase of $p_{initial}$ as a function of T_a is representative of an increasing number of denser domains. Since the mobility of the TPP molecules in these domains is drastically reduced compared with the surrounding supercooled liquid, the growth of phase

(63) Ha, A.; Cohen, I.; Zhao, X.; Lee, M.; Kivelson, D. *J. Phys. Chem.* **1996**, *100*, 1−4.

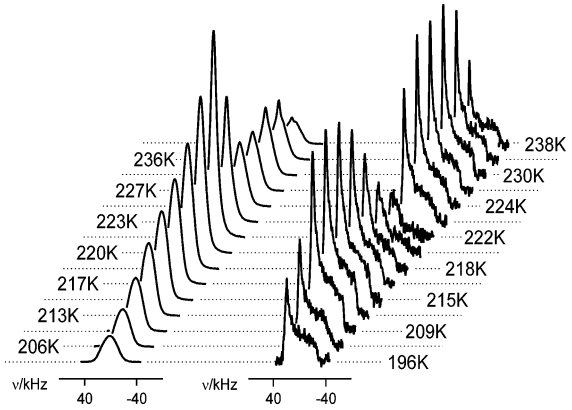

Figure 4. ^{1}H (left) and ^{31}P (right) solid-state NMR spectra recorded while heating a sample of TPP continuously at 0.3 K/min.

aII will probably be an interplay of molecules at the domain boundary and is thus relaxation driven. The resulting order of phase aII may then be a mean value of the order in the initially formed denser parts and in the supercooled liquid. Thus, the larger the p_{initial}, the higher the resulting order of phase aII will be.

Although the completely transformed phase aII is regarded as amorphous from X-ray diffraction, several groups suggested that the resulting structural order of phase aII exhibits periodic properties. Hédoux and co-workers[4,5,45,46] believe that phase aII is a mixture of supercooled liquid and nanocrystalline material, whereas Kivelson et al.[10] consider phase aII as a nanocrystalline plastic crystal. Furthermore, Tarjus and Alba-Simionesco as well as Kivelson[3,49] describe phase aII as a highly defect-ordered crystal as expected from their theory of frustration limited domains.[3] One central argument in this context is the premelting reported for phase aII while continuously heating this phase with a rate of 0.3 K/min.[10] The heating process was followed by measuring ^{1}H wide-line NMR spectra, and Kivelson et al. observed that directly preceding the crystallization of phase aII a sharp liquidlike resonance occurs in the ^{1}H spectra.[10] This signal was interpreted as a premelting and concluded that phase aII must exhibit translational order.

However, this signal may also be caused by a mobility of the phenyl rings of the TPP molecules. As Hédoux et al.[64] recently demonstrated by means of ^{2}H NMR line shape analyses phenyl rings in TPP perform fast 180° jumps about the OC-bond. Altogether the tumbling of whole molecules in the sample was not unambiguously proven and remained questionable at least. We therefore repeated the experiment of Kivelson but collected ^{31}P wide-line spectra in addition to ^{1}H experiments during the heating process. ^{1}H spectra are influenced by dynamical processes of both the side groups and the whole molecule, and ^{31}P line shape analyses exclusively probe molecular reorientations. Figure 4 displays the ^{1}H and ^{31}P wide-line spectra measured while heating a sample of glassified TPP continuously with a rate of 0.3 K/min. With increasing temperature the sample passes through the supercooled liquid, phase aII and the crystalline phase one after the other. As was mentioned above, the temperature region 227 K $\leq T \leq$ 236 K where phase aII starts crystallizing is of particular interest. In agreement with the experiment of Kivelson et al.,[10] the ^{1}H

(64) Lefort, R.; Hédoux, A.; Guinet, Y.; Cochin, E.; Descamps, M. *Eur. Phys. J. B* **2002**, *30*, 519−525.

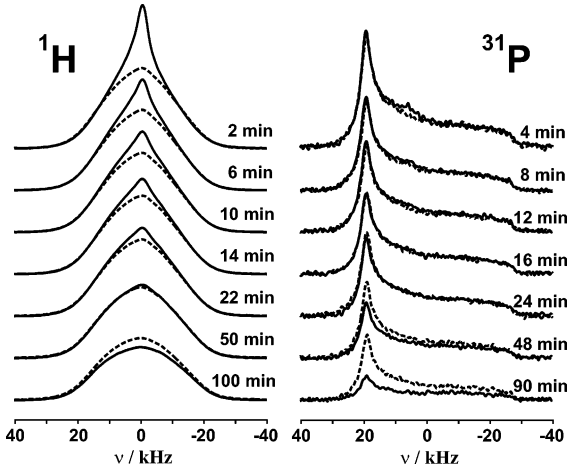

Figure 5. ^{1}H (left) and ^{31}P (right) solid-state NMR spectra recorded after heating two samples of phase aII quickly to 231 K. The first sample was annealed at $T_a = 218$ K (solid lines), whereas the second one was aged at $T_a = 225$ K (dashed lines).

spectra in this region clearly show a superposition of a sharp liquidlike and broad solidlike resonance. In contrast, the ^{31}P spectra can be described by a single broad resonance which is characteristic for rigid molecules and do not exhibit a sharp liquidlike resonance (right part of Figure 4).

This effect is even more pronounced if phase aII is prepared at low annealing temperatures ($T_a < 220$ K) and afterward heated quickly (20 K/min) to 231 K. Figure 5 shows the dependence of the ^{1}H and ^{31}P spectra collected for two samples annealed at $T_a = 218$ and 225 K as a function of time. Directly after heating to 231 K the ^{1}H spectra collected for the sample annealed at 218 K exhibit a pronounced sharp resonance, which disappears within roughly 20 min. Neither for the ^{1}H spectra recorded with the sample annealed at $T_a = 225$ K nor for the ^{31}P spectra acquired for both annealing temperatures (right part of Figure 5) an analogous behavior could be observed. For $t >$ 50 min the intensities of both the ^{1}H and ^{31}P spectra reduce indicating a slow formation of microcrystalline material with long T_1.

Two conclusions can be drawn from the line shape analyses of the 1D spectra. First, since no liquidlike resonance was observed in the ^{31}P spectra, the narrow part of the ^{1}H signal is caused by a side group mobility which is fast on the NMR time scale. Consequently, we could not confirm the premelting of phase aII. Second, the sharp resonance was not observed for the samples annealed at $T_a = 225$ K. Taking into account the results of the spin−lattice relaxation experiments discussed above, this strongly indicates a substantial difference for the structural order of phase aII annealed at temperatures above or below 223 K.

To obtain further insight into this topic we investigated the structural details of both amorphous phases by means of ^{31}P rf-driven spin-diffusion 2D exchange spectroscopy. As a function of the mixing time t_m we collected 2D spectra for the supercooled liquid as well as for phase aII prepared at different annealing temperatures T_a. For comparison, 2D spectra of the stable crystalline phase were also measured. All spectra were acquired at 190 K, where large angle reorientations of the TPP molecules are quenched[14] in all three phases to avoid any influence of molecular dynamics on the exchange spectra. The occurrence of cross intensity in the 2D spectra is therefore purely

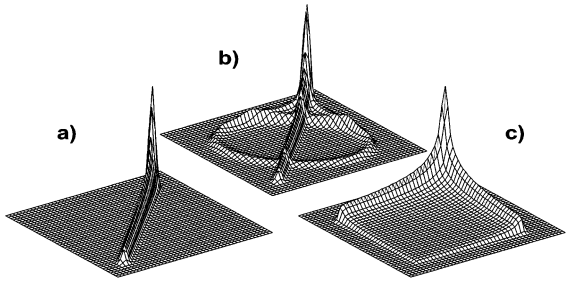

Figure 6. Simulated ^{31}P rf-driven spin-diffusion exchange spectra for $t_m \rightarrow \infty$ and different structural scenarios. (a) Parallel aligned molecules, (b) molecules in a fixed orientation of 50° toward each other, and (c) molecules with a random orientation.

based on spin diffusion and contains information about the arrangement of neighboring molecules. As demonstrated in detail in refs 39 and 53, the shape $S(\omega_1, \omega_2; t_m)$ of a 2D spectrum can be interpreted as the conditional probability $p(i, t_m|j, 0)$ of finding polarization, which is located on the phosphorus atom of molecule j in the first evolution period of the pulse sequence and on the phosphorus atom of molecule i in the second evolution period after a mixing time t_m. Since the orientation Ω of the TPP molecules is directly connected to the resonance frequency[39] ω, the occurrence of cross-peaks at the positions $S(\omega_i, \omega_j)$ and $S(\omega_j, \omega_i)$ proves the vicinity of molecule i with orientation Ω_i and molecule j with orientation Ω_j.

Depending on the local arrangement of the TPP molecules, the shape of a 2D spectrum varies. Figure 6 demonstrates typical 2D powder spectra in the limit $t_m \rightarrow \infty$ for three different structural scenarios. Figure 6a displays a spectrum which is typical for either isolated or parallel aligned molecules. In the former case, the coupling constant approaches zero and no exchange is possible. In the latter case the tensors of the anisotropic part of the chemical shift interaction are aligned parallel. Then ω_i and ω_j are identical for all powder increments, and no exchange is visible in a 2D spectrum. If the molecules have a set orientation relation, which is typical for crystals, for example, the shape of the cross intensity of the 2D spectra is composed of one or more elliptical ridges as shown in Figure 6b. The 2D spectrum shown in Figure 6c represents a random orientation of neighboring molecules typical for glasses or disordered materials. In this case a molecule with orientation Ω_i is correlated with equal probability to molecules in any other orientation. Thus, the frequency ω_i is correlated to every frequency of the 1D spectrum after mixing. The 2D exchange spectrum then results in a two-dimensional convolution of a 1D spectrum. The intensity is spread out over the whole 2D plane and displays a boxlike shape.

The perturbation approach which allows the expression of $S(\omega_1, \omega_2; t_m)$ in terms of the conditional probabilities $p(i, t_m|j, 0)$ requires that the dipolar coupling constants under spin-locking conditions ($b_{ij}^{eff} = s \cdot b_{ij}$) are smaller than the homogeneous line width of $F_{rf}(\omega)$. In the case of the TPP phases the maximal b_{ij}^{eff} is about 300 s^{-1} corresponding to a nearest neighbor distance of $d_{PP} = 6$ Å. Using the approach described in section 2, the homogeneous line width of $F_{rf}(\omega)$ turned out to be in the order of 600 s^{-1}, which is at least twice as large as b_{ij}^{eff}. The polarization transfer can be described using a master equation containing the exchange rates W_{ij} of the nuclei i and j with $W_{ij} \propto F_{rf}(0) \cdot r_{ij}^{-6}$. For reasons given in section 2, $F_{rf}(\omega)$ is expected to be constant for all spin pairs for the three phases of TPP. W_{ij} becomes proportional to $1/r_{ij}^6$ with r_{ij} being the distance between both nuclei. It should be noted, however, that if $F_{rf}(\omega)$ is not homogeneous, which would be the case if a material contains isolated strongly coupled spin pairs, for example, $F_{rf}(\omega)$ would also scale with r_{ij}^{-3} rendering $W_{ij} \propto 1/r_{ij}^3$.

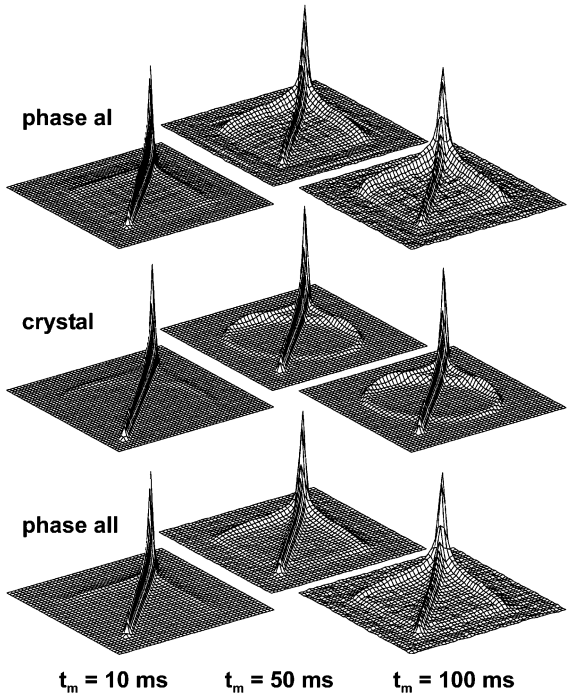

Figure 7. Comparison of ^{31}P rf-driven spin-diffusion exchange spectra for both amorphous phases and the crystal as a function of the mixing time.

For finite t_m the r_{ij} dependence of the exchange rates W_{ij} enhances the influence of the shorter molecular contacts on $S(\omega_1, \omega_2; t_m)$. This dominance becomes stronger when a shorter t_m is chosen. In other words, with a longer t_m, the volume becomes larger, which is investigated by the spin-diffusion process. Assuming a spherical probe volume and an isotropic spin diffusion, the order of the distance r_p over which the polarization can be transported within a given time t_m can be estimated by the following relation: $r_p = \sqrt{t_m \cdot \langle W \rangle} \cdot d$.[65] $\langle W \rangle$ denotes the mean exchange rate for all crystallite orientations, and d is the nearest neighbor distance between two TPP molecules. With $d = 6$ Å, $\langle W \rangle$ is in the order of 200 s^{-1} during the composite pulse spin-lock. Due to experimental problems such as insufficient dissipation of the rf-energy for long spin-locks, t_m is limited to a maximum value of about 200 ms. Within this time the polarization is transported over 6 to 7 molecules which corresponds to 35 Å $\leq r_p \leq$ 40 Å. By reducing t_m, r_p decreases which gives us the possibility to analyze the orientation correlation as a function of r_p. For a short t_m, only the strongest dipolar couplings take part in the exchange process and the 2D spectra turn out to be a direct image of the first coordination sphere.

Figure 7 shows a set of 2D exchange spectra for the structural glass, phase aII and crystalline modification of TPP for a short, middle, and long t_m, respectively. Phase aII was prepared by annealing the supercooled liquid at $T_a = 217$ K for 24 h. Even at first glance, it becomes obvious that both amorphous phases exhibit a similar shape of the cross intensity for all three mixing times, whereas the crystal results in a completely different shape.

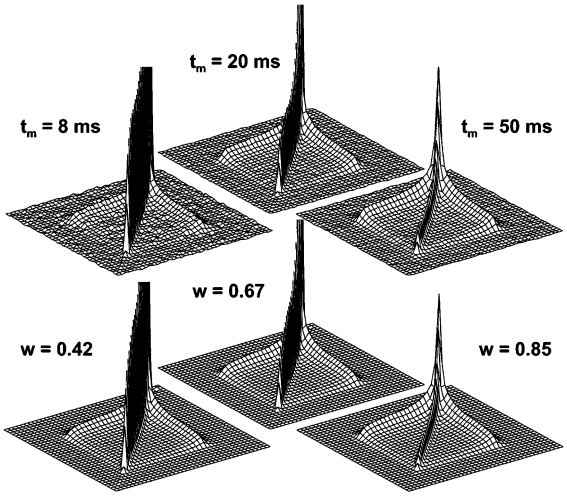

Figure 8. Experiment (upper part) and simulation (lower part) of 2D exchange spectra of the supercooled liquid. The parameter *w* represents the weighting factor for the superposition of the diagonal and cross part of the 2D spectra.

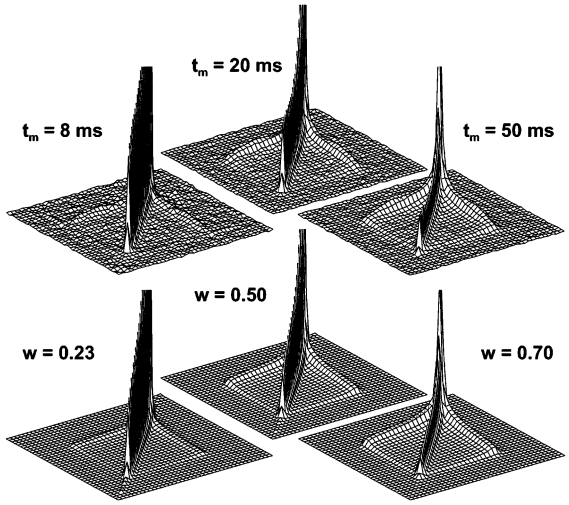

Figure 9. Experiment (upper part) and simulation (lower part) of 2D exchange spectra of phase aII prepared at $T_a = 217$ K. The parameter *w* represents the weighting factor for the superposition of the diagonal and cross part of the 2D spectra.

The latter is typical for a set orientation of neighboring TPP molecules (see Figure 6b).

The crystal structure of TPP[38] can be described as a hexagonal rod packing of TPP molecules. The molecules of one rod are aligned parallel and exhibit a PP distance of 5.76 Å. To minimize the net dielectric moment, neighboring rods are ordered in an antiparallel way leading to a trigonal space symmetry.

Since the molecules in a single rod are aligned parallel, they do not contribute to the cross intensity of the exchange spectra.[38,39] The ridgelike shape of the cross intensity (see Figure 7) is caused by neighboring molecules from different rods.[38,39] These molecules are arranged according to a $\bar{3}$ rotoinversion axis, and their phosphorus atoms form a strongly distorted octahedron with a shortest PP distance of 8.09 Å.[38] Thus, one should bear in mind that the occurrence of a ridgelike shape as depicted in the middle part of Figure 7 is characteristic for the formation of antiparallel aligned rods of TPP molecules.

In contrast, the cross intensity of 2D spectra recorded for the structural glass is spread out over the whole 2D plane and exhibits a boxlike shape for all three mixing times (see Figures 7 and 8). This is typical for molecular glasses where neither the orientation nor the distances of neighboring molecules exhibit strong structural correlations.[66] To be able to exclude even weak orientational correlations which would lead to subtle changes of the 2D spectra, we also simulated exchange spectra for an ensemble of uncorrelated molecules. In this case, the transfer of polarization from one molecule to another always leads to a loss of correlation, and the 2D spectra can be simulated by a simple superposition of a diagonal spectrum with an intensity I_D (Figure 6a) and a boxlike spectrum with an intensity I_C (Figure 6c). The weighting factor $w = I_C/I_D$, which depends on t_m, is the only parameter of freedom and describes how much polarization has already been transferred to the surrounding nuclei.

Figure 8 depicts experimental and simulated 2D spectra of the structural glass prepared by cooling the liquid rapidly to 190 K for three different mixing times. The cross part of the simulated exchange spectra, showing the boxlike shape representative for an uncorrelated orientation of neighboring molecules, was created by performing a two-dimensional convolution of a 1D ^{31}P NMR spectrum. For long as well as for short t_m, the agreement between the experiment and the simulation is excellent. While $t_m = 50$ ms corresponds to a polarization transfer over a distance of $r_p \approx 20$ Å, a t_m of 8 ms is only representative for the first coordination sphere ($r_p \approx 8$ Å). As is expected for a molecular van der Waals glass, these results confirm the absence of an orientation correlation for short and intermediate lengths in phase aI. Combined with the observations for the crystalline phase,[38,39] it has been demonstrated that rf-driven spin-diffusion exchange spectroscopy is suited to probe orientational order as well as disorder quite accurately.

Therefore, this method is also applicable to the investigation of structural properties of phase aII, and we performed a similar analysis for several samples annealed in the temperature range $212\ \text{K} \le T_a \le 227\ \text{K}$ for up to 2 d. After each completed transformation, the data collection was carried out at 190 K and took roughly 20 h for one 2D spectrum. For $T_a < 220$ K, the 2D spectra are almost identical and do not change as a function of T_a. Figure 9 shows three examples of spectra for a sample annealed at $T_a = 217$ K. These spectra demonstrate that in this temperature range the same arguments outlined for the structural glass also hold for phase aII. Again the shape of the cross intensity is typical for an uncorrelated orientation of neighboring molecules with short and intermediate distances (see Figure 7). The comparison with our simulations reveals a pretty good agreement (see Figure 9). No indications for even weak orientational correlations could be observed, neither for the first ($t_m = 8$ ms) nor for larger ($t_m > 50$ ms) coordination spheres. The strong similarity of the behavior of the exchange spectra measured for the structural glass and phase aII gives strong evidence that both phases have similar structural properties. However, for phase aII the systematically smaller weighting factors *w* indicate the shortest mean PP distance between

(65) Abragam, A. in *Principles of nuclear magnetism*, chapter4, p 139. Oxford Science Publications: Oxford, 1961.
(66) Böhmer, R.; Diezemann, G.; Hinze, G.; Rössler, E. *Prog. Nucl. Magn. Reson. Spectrosc.* **2001**, *39*, 191−267.

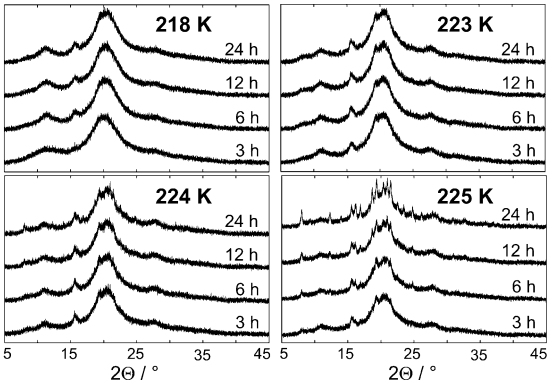

Figure 10. X-ray powder pattern for the transformation of the supercooled liquid into phase aII at different annealing times and temperatures.

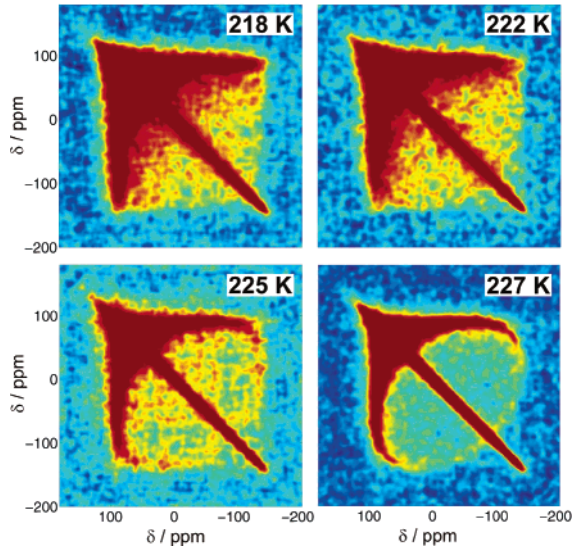

Figure 11. ^{31}P 2D exchange spectra (t_m = 120 ms) of phase aII prepared by annealing the supercooled liquid at different temperatures for 24 h. The spectra were collected after cooling the annealed sample to 190 K.

neighboring TPP molecules to be somewhat larger in comparison with the structural glass. We will deal with this point later.

First of all, we will discuss the structural properties of phase aII for larger annealing temperatures (T_a > 220 K). For various T_a X-ray diffraction data were recorded in addition to the ^{31}P exchange spectra. According to the 2D spectra the samples were annealed at a constant temperature for up to 24 h. During this time we continuously collected diffraction data and were able to follow the transformation process as a function of the annealing time. Figure 10 shows examples of the diffraction patterns for four different T_a and annealing times. The appearance of a small prepeak at 2Θ = 15.7° shows the formation of phase aII in agreement with the literature.[11,67] Whereas phase aII appears radiographically amorphous for $T_a \leq$ 220 K, a nanocrystalline material starts to develop for T_a at around 224 K.

The appearance of the ^{31}P 2D spectra measured for different annealing temperatures match these observations (see Figure 11). As has already been mentioned above, the shape of the cross intensity for spectra recorded for $T_a \leq$ 220 K is characteristic for an absence of orientational correlations of

(67) Hédoux, A.; Guinet, Y.; Descamps, M.; Hernandez, O.; Derollez, P.; Dianoux, A. J.; Foulon, M.; Lefèbvre, J. *J. Non-Cryst. Solids* **2002**, *307*−*310*, 637−643.

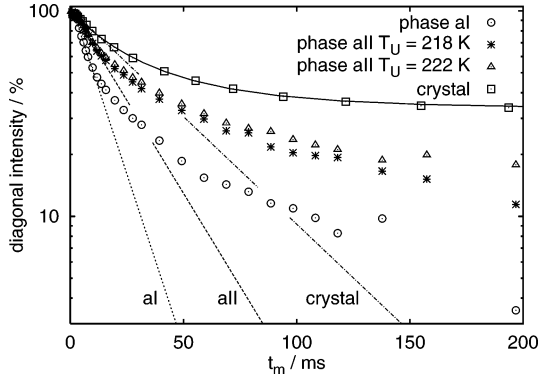

Figure 12. Diagonal intensity I_D of 2D exchange spectra for both amorphous phases as well as the crystalline modification as a function of t_m. For phase aII two different annealing temperatures are included. The solid line denotes the result of a simulation for the crystalline phase containing 300 molecules within a sphere with a radius of 30.5 Å.[39] The dashed and dotted lines represent linear fits to the initial regime of I_D to determine the initial slope dI_D/dt_m.

neighboring TPP molecules. Even though subtle, at T_a = 222 K for the first time the cross intensity shows deviations from this spectral shape. The changes are most obvious in the upper right and lower left regions of the spectrum. For the 2D spectra collected at 225 K (see Figure 11), these deviations are more pronounced and a ridgelike shape typical for the crystal starts to develop. However, the ridge is broadened and the cross intensity is smeared out over the whole 2D plane. In contrast, the spectra acquired at 227 K exhibit a quite sharp ridge and resemble the spectra recorded for the crystalline phase (see Figure 7). In accordance with the diffraction data as well as the ^{31}P spin−lattice relaxation measurements and 1D spectra collected during the heating experiments, these observations can be interpreted as an onset of crystallization of phase aII within 222 K $\leq T \leq$ 224 K. Whereas at 225 K the size of the crystallites is in the order of a few nanometers, a well developed microcrystalline material is formed at 227 K.

Up to now the discussion has been restricted to the shape of the 2D spectra, which provides information about the orientation correlation of neighboring molecules. By additionally using the t_m dependence of a series of 2D spectra, an estimation about the distances between these molecules can be made. For the crystalline phase of TPP as a model compound, we recently simulated the decay of the integral diagonal intensity $I_D(t_m)$ for confined spin systems for up to 300 phosphorus nuclei.[39] In systems with more than 10 spins the P atoms were selected from the crystallographic data[38] by locating the atoms in a sphere with the radius r_s around the inversion center in the middle of the unit cell. The curve of $I_D(t_m)$ quickly converges with increasing r_s and does not change for r_s > 27 Å, which corresponds to 210 TPP molecules. The solid line displayed in Figure 12 represents a simulation for r_s = 30.5 Å (300 molecules). The agreement between the simulation and the experimental data is excellent and demonstrates that rf-driven spin-diffusion exchange spectroscopy can be used to probe the validity of a given structure model.

However, to generate a structure model with a few hundred molecules is easy only for crystalline phases. In the case of TPP, one molecule is located in the asymmetric unit and thus only five parameters, the fractional coordinates *x*, *y*, and *z* as well as the lattice parameters *a* = *b* and *c*, have to be taken

Table 1. *R*, $F_{rf}(0)$, *g*, and d_g Are Listed for the Structural Glass, Two Samples of Phase aII Annealed at Different T_a and the Crystalline Modification[a]

	aI	aII		crystal
		$T_a = 218$ K	$T_a = 222$ K	
R/s^{-1}	−78.7(6)	−49.6(6)	−50.7(6)	−36.2(5)
$F_{rf}(0)/\times 10^{-3}$ s	1.44(4)	1.62(4)	1.60(4)	1.52(4)
$g/\times 10^{+55}$ m^{-6}	3.64(9)	2.04(7)	2.11(7)	1.59(5)
d_g/Å	5.29	5.83	5.80	6.08

[a] *g* was calculated from the experimental data using eq 5 and d_g results from eq 7 to $d_g = \sqrt[6]{4/(5g)}$.

into account to build up a phosphorus spin system of any size.[39] In contrast, for the amorphous phases the generation of realistic structure models is a much more elaborate task usually requiring MD or MC simulations.[21−23,29] Due to the large number of parameters of freedom for one TPP molecule, such simulations would already go beyond the scope of the work presented here. We therefore restrict our analysis to the initial rate regime, where the slope *R* of $I_D(t_m)$ can be interpreted as

$$R = \frac{dI_D}{dt_m} = -\frac{{\mu_0}^2\gamma^4\hbar^2}{128\pi} \cdot s^2 \cdot F_{rf}(0) \cdot g \qquad (5)$$

with *g* denoting the geometrical factor[52] containing the structural information.

The central element of *g* is the sum over the angle and distance dependent parts of the dipolar coupling constants of a probe nucleus j to all other spins of the ensemble with the condition $\omega_j \neq \omega_i$. ω_j and ω_i are the CSA dominated resonance frequencies of the spins j and i. This condition states that spins with equal resonance frequencies although coupled do not lead to a net polarization transfer. *g* is afterward calculated by performing the ensemble average over the probe nucleus resulting in

$$g = \left\langle \sum_i \frac{(3\cos^2\vartheta_i - 1)^2}{r_i^6} \right\rangle \qquad (6)$$

r_i denotes the distance between the probe nucleus and spin i, and ϑ_i is the angle between the external magnetic field $\vec{B}_0$ and $\vec{r}_i$. If ϑ_i and r_i are uncorrelated, *g* can be simplified to

$$g = \sum_i \frac{\langle(3\cos^2\vartheta_i - 1)^2\rangle}{\langle r_i^6\rangle} = \frac{4}{5} \cdot \langle \sum_i r_i^{-6}\rangle = \frac{4}{5} \cdot d_g^{-6} \qquad (7)$$

To determine *g* for both amorphous phases as well as for the crystalline modification we extracted the slope *R* from linear refinements of $I_D(t_m)$ in a semilogarithmic plot as given in Figure 12. $F_{rf}(0)$ was probed independently as described in section 2 by measuring the magnetization decay after a Hahn-echo for varying interpulse distances. *R*, $F_{rf}(0)$, *g*, and $d_g = \langle \Sigma_i r_i^{-6}\rangle^{-1/6}$ as determined for all three phases are given in Table 1. d_g can be used as a measure for the closeness of neighboring spins, which participate with the net polarization transfer.

The geometrical factor *g* is largest for phase aI and smallest for the crystalline phase of TPP (see Table 1). The *g* of phase aII is positioned between and exhibits no significant dependence on the annealing temperature if phase aII is prepared below 223 K. It should be noted that *g* of phase aII is significantly closer to the crystalline phase than to the structural glass. The value of 1.59×10^{55} m^{-6} determined for the crystalline phase agrees well with simulations of *g* based on the crystallographic data, resulting in 1.607×10^{55} m^{-6} ($r_s = 30.5$ Å). Although ϑ and *r* are not strictly uncorrelated in the crystalline phase of TPP, $d_g = 6.08$ Å derived from eq 7 fits nicely the simulated value 6.062 Å demonstrating that d_g can be used to compare structural properties of all three phases. It should be noted here for the following discussion that since d_g contains the sum over all inverse distances relative to a probe nucleus, the distance d_g is significantly shorter than the shortest value in the real structure. For example, the shortest PP distance, which participates in the net polarization transfer in the crystalline structure, is 8.09 Å, whereas d_g is equal to 6.08 Å. This corresponds to a factor of 1.32.

$d_g = 5.29$ Å determined for the structural glass is by 13% smaller compared to the value derived for the crystalline phase (see Table 1). This effect can most probably be assigned to the fact that in phase aI even neighboring TPP molecules exhibit a random orientation and, thus, all molecules contribute to a net polarization transfer. By applying the factor 1.32 to the structural glass, the shortest mean PP distance is calculated to be ∼6.9 Å. However, this is only a rough estimate, as the structure of phase aI differs significantly from the packing in the crystalline phase which the factor used is derived for. Nevertheless, taking into account that the crystal is denser than phase aI,[10] this value may still be reasonable, since the shortest PP contact in the crystalline phase is 5.76 Å between parallel aligned molecules of one rod.[38]

Although the similar shape of the 2D spectra for both amorphous phases indicates analogous structural features for phases aI and aII, $d_g = 5.8$ Å measured for phase aII is larger by 11% compared to the value observed for phase aI. Applying again the factor 1.32, the shortest mean PP distance in phase aII should be estimated to be around 7.5 Å. Two effects may explain this larger value: First, if the transformation of the supercooled liquid into phase aII is driven by conformational changes of the TPP molecules as was proposed earlier,[8] the increase may be caused by a lower-density packing due to a different average shape of the TPP molecules in phase aII. This argument, however, is contradicted by the higher density of phase aII.[10] Second, if phase aII contains small clusters of parallel aligned molecules, each cluster consisting of only a few molecules, the PP distances between these molecules do not contribute to d_g, since those molecules always have the same resonance frequency. Thus, d_g would increase although the molecules are packed more densely than in phase aI.

The second scenario is further supported by analyzing the initial spin-diffusion rate constants as a function of different ^{31}P chemical shielding pairs. Figure 13 depicts the rate constants in the full cross-peak region for the structural glass, phase aII with $T_a = 217$ K and phase aII with $T_a = 222$ K. In a structurally disordered material without orientational correlations (even on a short range) the rate constants should be the same for all cross-peaks. Within the range of accuracy this condition holds for the structural glass of TPP (left part of Figure 13). The plot of the initial rate constants shows a flat rate profile demonstrating

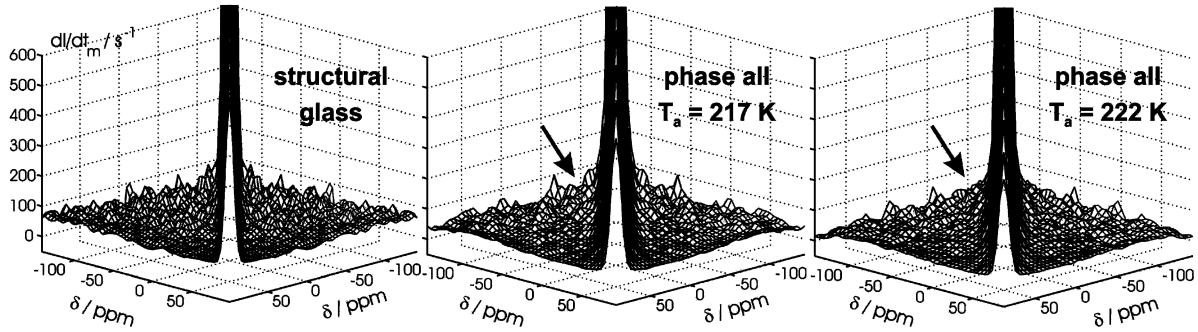

Figure 13. Initial spin-diffusion rate constants as a function of different ^{31}P chemical shielding pairs for both amorphous phases of TPP. They were extracted as $S(\omega_1, \omega_2;12ms)/S(\omega_1, \omega_2;\infty)$. $S(\omega_1, \omega_2;12ms)$ represent the experimentally observed 2D exchange spectra collected at t_m = 12 ms normalized to unit intensity. The $S(\omega_1, \omega_2;\infty)$ for infinite mixing times were simulated for a random orientation of neighboring molecules as described in the text on page 15 and are also normalized. For the analysis of the rate constants only the full cross-peak region has to be considered. The diagonal part is obscured by polarization, which does not yet take part in the exchange process.

that the bandwidth of the composite spin-lock is broad enough to cover the whole 1D spectrum. For both samples of phase aII, however, the cross-peaks near the diagonal grow faster (arrows in Figure 13) than all other cross-peaks. Since cross-peaks near the diagonal are representative for almost parallel aligned TPP molecules, the data depicted in the middle and right part of Figure 13 imply that phase aII indeed consists of small clusters of preferentially parallel aligned molecules. The mean distance of these molecules is somewhat smaller than that between orientationally uncorrelated molecules.

4. Discussion

Based on the results of the 1D and 2D solid-state NMR experiments and X-ray powder diffraction data presented here, phase aII appears to be homogeneous and disordered on local and intermediate length scales if prepared by annealing the supercooled liquid below 223 K. In the beginning of the transformation the samples turn out to be heterogeneous. Therefore it is essential to choose sufficiently long annealing times. Since the homogeneity is a controversial topic in the literature,[1,2,4,9] we used two different techniques to probe structural heterogeneities of phase aII. ^{31}P spin−lattice relaxation indirectly maps the local arrangement of the TPP molecules by probing their local molecular dynamics. ^{31}P rf-driven spin diffusion is a direct measure of the orientation correlation of neighboring molecules. Both techniques are sensitive to order phenomena in a confined probe volume and thus are suited to detect heterogeneities, even on a local scale.

The relaxation function $\Phi(t)$ (see Figure 2) and the shape of the exchange spectra of the phase aII (see Figures 7 and 11) show very similar behavior to the one measured for the structural glass, which is unanimously considered to be a homogeneous phase. Thus, up to an annealing temperature of $T_a \approx 223$ K our experimental data do not support any description of phase aII as a domain structure where the individual domains exhibit different degrees of structural order. Although our results agree with the propositions of most other groups[1−3,9,10,14−16] working on TPP, they contradict the picture of phase aII which describes it as a mixture of a disordered phase (like the supercooled liquid) and nanocrystalline material.[4−6,44−47] In this case, the relaxation function $\Phi(t)$ is expected to be biexponential, and the 2D spectra should be a superposition of the spectra acquired for phase aI and the ordinary crystal.

For annealing temperatures $T_a > 223$ K the relaxation behavior, the shape of the X-ray diffraction pattern and the 2D spectra change markedly, demonstrating that depending on T_a either a nano- or a microcrystalline material is formed. The behavior of ^{1}H and ^{31}P 1D spectra collected as a function of time after heating phase aII quickly to 231 K also points in the same direction (see Figure 5). If prepared at 218 K the ^{1}H spectra of phase aII exhibit a sharp liquidlike resonance directly after heating to 231 K, which vanishes within roughly 20 min. In contrast, for $T_a = 225$ K no such resonance could be observed. Consequently, the structural properties of phase aII annealed at 218 K differ from those annealed at 225 K. At this temperature the exchange spectra as well as X-ray diffraction pattern already reveal a nanocrystalline material.

Since no liquidlike resonance could be observed in the ^{31}P spectra (see Figure 5), the effect described above is caused by a mobility of the side groups only. Among other processes the side group mobility incorporates 180° jumps of the phenyl rings about their 2-fold axis. Such reorientations were recently observed by Hédoux et al.[64] in the course of the transition into phase aII. After an increase in temperature, the disappearance of the liquidlike resonance well before an initiation of crystallization ($t > 50$ min) indicates that the TPP molecules of phase aII relax into a more stable arrangement where the overall side group mobility is reduced. Rössler et al.[14] derived mean correlation times in the order of a few hundred seconds for the α-relaxation in the relevant temperature region of 210 K $\leq T_a \leq$ 220 K which corresponds to a fairly high viscosity. Besides the α-relaxation, the mobility of the side groups, which allows the TPP molecules to change their conformation, provides an additional mechanism for structural relaxation. Probably both relaxation mechanisms are responsible for the decay of the density fluctuations in the final stage of the transition. These fluctuations, found by Tanaka et al.[1] using optical microscopy, are in good agreement with the biexponential relaxation observed in the present work in the initial regime of the transformation, whereas the decay of the heterogeneous areas is matched by the slow assimilation to one uniform T_1.

The idea that the arrangement of the TPP molecules of phase aII is a function of the annealing temperature T_a is further supported by the behavior of the mean spin−lattice relaxation constants $\langle T_1 \rangle$ (see Figure 3). Measured at 200 K, $\langle T_1 \rangle$ increases with increasing T_a which denotes a reduction of the local mobility of the TPP molecules. This could simply be either an

effect of a denser packing or, as Oguni and co-workers[16] proposed from their calorimetric investigations, the development of a state of increasing order as a function of T_a. However, it should be noted that due to the analysis of the 2D exchange spectra, the resulting order has to be different from the symmetry established in the crystalline phase.

A detailed analysis of the rf-driven polarization transfer as a function of t_m (see Figures 8 and 9) unambiguously shows that neighboring molecules in both amorphous phases have to be either orientationally uncorrelated or aligned parallel on local and intermediate scales. The geometrical factor and $d_g = 5.3$ Å determined for the structural glass lead to reasonable nearest neighbor PP distances of ~6.9 Å for randomly distributed TPP molecules. This agrees with the flat rate profile of the initial rate constants (Figure 13) which imply the absence of orientational correlations in the first coordination sphere. Thus, as expected for an ordinary molecular glass, no local structural correlations were observed. $d_g = 5.8$ Å of phase aII is placed between the values determined for phase aI and the crystalline phase ($d_g = 6.1$ Å) and is, however, closer to the value of the crystalline modification. An analysis of the initial rate constants in phase aII demonstrates that independent of the annealing temperature (T_a = 217 K, 222 K) the cross-peaks near the diagonal grow faster than all other cross-peaks. Both results strongly favor the formation of small clusters of preferentially parallel aligned TPP molecules.

In addition, on considering that the local disorder, probed by analyzing the reorientational dynamic of a small probe molecule, is similar in both amorphous phases,[8] the clusters must be spatially separated. The loss of the diagonal intensity I_D to below 10% of its original value for large t_m and $T_a = 218$ K (see Figure 12) indicates that the cluster size is limited to a few molecules. The independence of d_g from the annealing temperature T_a further shows that the size of these clusters does not change significantly with T_a. Therefore, an increase in $I_D^{t_m \to \infty}$ ($I_D \approx$ 18% at T_a = 222 K) indicates an increase in the number of clusters.

The existence of clustered parallel aligned molecules as well as the increasing number of clusters as a function of T_a result in a higher degree of correlations as a function of T_a and agrees with the proposition of Oguni et al..[16] It also explains the behavior of the optical birefringence observed by Tanaka et al.[1] without assuming a mixture of phase aII and microcrystallites, which is not consistent with the results presented here of the spin−lattice relaxation and rf-driven spin-diffusion experiments. The same arguments also hold for the Raman data collected by Hédoux et al.[4,5,45−47] from which the authors derived their picture of phase aII as a mixture of the supercooled liquid and nanocrystallites. If the arrangement of the TPP molecules within the clusters resembles that of the rods of the crystalline phase, the Raman spectra will develop a signature similar to the one found for the crystal, even without the antiparallel alignment of rods of molecules. It is this alignment though which defines the translational symmetry of the crystalline phase and therefore is essential for the formation of crystal nuclei.

The existence of small clusters of parallel aligned molecules furthermore explains the unusually stretched correlation function for the reorientational dynamics of the TPP molecules of phase aII observed by Rössler and co-workers.[14] Depending on the number of molecules in a single cluster, its correlation time τ will be slowed accordingly leading to a broad distribution of τ. Since the analytical methods applied in the work presented here are limited to an intermediate scale of roughly 30−40 Å, we did not address order phenomena on larger scales. Thus the results of Alba-Simionesco, Tarjus, and Kivelson[2] indicating a poorly developed mesoscopic order on a scale of 80−200 Å are not contradictory, particularly because the authors do not comment on the local structural properties of phase aII. Probably the mesocopic order is a result of the unusual transformation behavior including the existence of an intermediate phase, which does not reflect the structural properties of either the supercooled liquid or phase aII.

5. Concluding Remarks

For the first time a detailed microscopic description of phase aII could be presented. It is consistent with most of the experiments carried out on the second amorphous phase of TPP by various groups in recent years. We describe phase aII as a homogeneous and disordered phase up to an annealing temperature of 223 K. The transformation of the supercooled liquid is driven by self-organization of a number of the TPP molecules into small clusters of parallel aligned molecules, which appear to be separated from each other. The number of molecules within one cluster probably varies, with its maximum size not exceeding a few molecules. Whereas the cluster size within the experimental error does not change, the number of clusters grows with increasing T_a. However, it is not until the number of clusters exceeds a certain limit and the viscosity of phase aII becomes low enough, allowing large angle reorientations of even the larger clusters, that the organization into the crystal is initiated by arranging the clusters into antiparallel aligned rods of TPP molecules.

In our opinion, the results presented here strongly suggest that phase aII can be described as a second liquid, where a part of the molecules exhibit structural correlations. However, the question about the origin of these correlations remains unanswered. Regarding the structure model described above, two scenarios have to be taken into account. First, since the clusters may resemble a part of the crystal structure, on a first look it might be reasonable to think of the cluster formation as an early stage of nucleation and thus as an onset of crystallization. In this case, both the number as well as the size of the nuclei should grow as a function of T_a. According to our experiments, however, the cluster size is independent of T_a. Furthermore, one has to keep in mind that the main characteristic of the crystal is the antiparallel ordering of the rods of molecules. Thus, it is at least questionable to regard small clusters of parallel aligned molecules as crystal nuclei. Combined with the large temperature range in which phase aII can be prepared without forming either a nano- or microcrystalline material, we think this scenario is less probable.

Second, the clusters may be regarded as a *locally preferred structure* (LPS) as proposed in the concept of Tarjus and Kivelson,[2,3] to explain the origin of the polyamorphism phenomenon. The authors think of transitions between two liquid or amorphous phases as a competition between different LPSs. This scenario it fully consistent with the structural description of phase aII that we have developed. However, since the process of the phase transformation includes density fluctuations in the

beginning, which results in an intermediate phase with structural and physical properties different from both the supercooled liquid and phase aII, this discussion remains somewhat speculative. To develop a better understanding of the thermodynamic and kinetic anomalies associated with this transformation, it is necessary to investigate the structural properties of the intermediate phase in more detail and to determine the arrangement of the TPP molecules within the clusters. At the moment we are working on both aspects using ^{13}C and ^{31}P double- and zero-quantum NMR experiments as well as force field methods.

JA046602Q